

Enhanced detection of Theiler's virus RNA copy equivalents in the mouse central nervous system by real-time RT-PCR

Mark Trotter^{a,b}, Brian P. Schlitt^{a,b}, Howard L. Lipton^{a,b,*}

^a Department of Neurology, Evanston Hospital, 2650 Ridge Avenue, Evanston, IL 60201, USA

^b Departments of Neurology, Microbiology-Immunology, and Biochemistry, Molecular Biology and Cell Biology, Northwestern University, Evanston Chicago, IL, USA

Received 13 August 2001; received in revised form 15 January 2002; accepted 16 January 2002

Abstract

Infection of mice by low-neurovirulence Theiler's murine encephalomyelitis virus (TMEV), such as BeAn and DA viruses, provides a relevant experimental animal model for multiple sclerosis (MS). As a step toward determining the kinetics of a persistent central nervous system (CNS) infection that leads to chronic demyelination, we adapted a rapid, accurate and highly specific real-time reverse transcriptase-polymerase chain reaction (RT-PCR) assay for detection and quantitation of BeAn virus RNA copy equivalents in mouse tissues. The assay enabled detection of as few as 20–30 copies of BeAn virus RNA per μg of total RNA from infected mouse tissues and results for spinal cord revealed the same high levels of BeAn RNA as detected by Northern hybridization during the first 4 months of the persistent infection, but also was able to detect virus RNA copies as late as 1 year post-infection. Real-time RT-PCR analysis of BeAn virus RNA copy equivalents in different parts of the CNS, analyses not possible by Northern hybridization, revealed the following cline of virus persistence: spinal cord > brainstem/cerebellum > cerebrospinal fluid (CSF) > cerebral hemispheres. Systemic organs, including heart, intestine and mesenteric lymph nodes of infected mice, showed no evidence of viral persistence at 4 months post-infection. © 2002 Elsevier Science B.V. All rights reserved.

Keywords: Theiler's virus; Persistent infection; Real-time RT-PCR; Virus RNA copies

1. Introduction

Theiler's murine encephalomyelitis virus (TMEV) is an enteric pathogen of mice that belongs to the *Picornaviridae* family (Pevear et al., 1987). Low-neurovirulence TMEV, such as the BeAn and DA viruses, cause a persistent infection

in the central nervous system (CNS) of susceptible mice that results in immune-mediated and viral damage to oligodendrocytes, and hence, demyelination (Blakemore et al., 1988; Gerety et al., 1994; Rodriguez et al., 1983; Clatch et al., 1986). Thus, infection of mice with the low-neurovirulence TMEV provides an experimental animal model that might be useful in understanding how a persistent CNS infection leads to chronic demyelination, such as might be the case in multiple sclerosis (MS).

* Corresponding author. Fax: +1-847-570-1568.

E-mail address: hlipton@merle.acns.nwu.edu (H.L. Lipton).

During the acute phase of viral growth, low-neurovirulence TMEV strains infect neurons in the gray matter of the brain and spinal cord (Aubert and Brahic, 1995; Simas and Fazakerley, 1996; Jarousse et al., 1998), followed by virus persistence in macrophages and glial cells in the spinal cord white matter. Persistence of TMEV in the mouse CNS has traditionally been demonstrated by the recovery of infectious virus from the spinal cord. Results of infectivity assays have led to the notion that TMEV persists only at low levels ($<10^4$ PFU detected per spinal cord) due to restricted infection and failure of viral clearance from the spinal cord (Lipton and Melvold, 1984; Chamorro et al., 1986). Northern hybridization has also been used for analysis of TMEV persistence (Bureau et al., 1992) and relative abundance of TMEV RNA in spinal cords from infected mice (Larsson-Sciard et al., 1997). Our own recent Northern dot blot analysis revealed large numbers of TMEV genomes in the spinal cord of persistently infected mice, with a mean level of 3.0×10^9 in tissues examined between pi days 30 and 223 (Trottier et al., 2001). However, Northern hybridization is labor-intensive and has a high detection threshold, i.e. at least 9×10^6 TMEV RNA genomes must be present, thus requiring large amounts of spinal cord total RNA (10 μ g) per reaction.

Here, we report the detection and quantitation of BeAn virus RNA copy equivalents in host tissues using a rapid, accurate and highly specific real-time reverse transcriptase-polymerase chain reaction (RT-PCR) assay. This method was standardized using *in vitro* transcribed BeAn virus RNA, and results of RT-PCR quantitation of virus RNA copy numbers were consistent with values determined by our previous Northern analysis (Trottier et al., 2001). The sensitivity of real-time RT-PCR, i.e. detection of as few as 20–30 copies of BeAn virus RNA per μ g of total RNA from infected mouse tissues, enabled quantitation of BeAn virus RNA copy equivalents in different parts of the CNS early in persistence and at late times pi, when virus RNA titers were expected to be below the detection limits of Northern hybridization. A hierarchy of sites of BeAn virus persistence in the CNS was revealed, whereas no

evidence of persistence was found in several extraneural sites examined.

2. Materials and methods

2.1. Virus stock

The maintenance of BHK-21 used to grow virus has been described (Jelachich et al., 1999). The titer of the plaque-purified stock of BeAn 8386 virus grown in BHK-21 cells monolayers was 6.6×10^6 PFU per ml. The passage history of BeAn 8386 virus has been described (Pevear et al., 1987).

2.2. Mice and virus inoculations

SJL female mice, purchased from The Jackson Laboratory (Bar Harbor, ME), were caged and maintained in accordance with American Association for Accreditation of Laboratory Animal Care standards, and received autoclaved standard mouse chow and water *ad libitum*. Mice (5–6 weeks old) were anesthetized by intraperitoneal (ip) injection of 1 mg pentobarbital and inoculated in the right cerebral hemisphere with 1×10^6 PFU of virus in 30 μ l. Age-matched control SJL mice were uninoculated.

2.3. Total RNA isolation

Mouse spinal cord [flushed from spinal canals with chilled PBS deficient in Ca^{++} and Mg^{++} without loss of cerebrospinal (CSF)], cerebrum (separated from brainstem and cerebellum by sectioning between the anterior cerebellum and colliculi dorsally to the interpeduncular fossa ventrally), cerebellum/brain-stem, and extraneural organs obtained at necropsy were snap-frozen in LN₂, placed between two clean plastic weight boats, broken into small pieces with a hammer that were transferred to a polypropylene tube and Trizol reagent (Gibco) was added (w/v). Tissue was homogenized with a Polytron homogenizer (Beckman Instruments), and total RNA was isolated according to the manufacturer's recommendations. The integrity of RNA from tissues of

individual mice was determined by visualization of 18- and 28S ribosomal RNA following agarose gel electrophoresis. On average, 700 µg of total RNA was extracted from the cerebrum ($n = 9$), 200 µg from the brainstem/cerebellum ($n = 14$) and 75 µg from the spinal cord ($n = 9$).

2.4. Northern hybridization

Total RNA from mouse tissues or cell cultures was ethanol-precipitated, resuspended in RNA loading buffer [50% formamide, 7% formaldehyde, 0.04% bromophenol blue in 200 mM 3-(N-morpholino)propanesulfonic acid, pH 7.0, 50 mM sodium acetate, 10 mM EDTA (MOPS buffer)], heated for 5 min at 95 °C, and electrophoresed in a 1% agarose gel at 80–90 V for 1 h, and hybridized to a random-primed DNA [α -³²P]dCTP-labeled probe specific for BeAn virus as described (Trottier et al., 2001).

2.5. Real-time RT-PCR

The TaqMan system (Applied Biosystems) is a fluorogenic probed-based PCR assay that exploits the 5' to 3' endonuclease activity of Taq polymerase. An oligonucleotide probe labeled with both reporter [6-carboxyfluorescein (6-FAM)] and quencher [6-carboxyethyltetramethylrhodamine (TAMRA)] dyes anneals to an internal region of PCR amplicons and is digested as Taq polymerase extends the PCR primer. The separation of reporter from quencher dyes leads to increased fluorescence.

Reverse transcription reaction mixtures contained differing amounts of total RNA (usually in the range of 0.05–2 µg plus carrier total brain RNA), with 1 × Taqman buffer, 5.5 mM MgCl₂, 0.5 mM dNTPs, 3.5 µM random hexamers, 0.4 U RNasin, and 1.25 U of Multiscribe reverse transcriptase (Applied Biosystems) in 10 µl. Mixtures were incubated at 24 °C for 10 min, 48 °C for 30 min and 95 °C for 5 min. Each 50-µl PCR reaction contained 3 µl of cDNA, and the final concentration of each component was: 0.5 × Taqman Gold Universal PCR master mix containing AmpliTaq Gold DNA polymerase, AmpErase uracil-N-glycosylase (UNG), and dUTP instead of

dTTP (Applied Biosystems); 2.5 pmol of forward and reverse primers; 1.5 pmol of TaqMan probe (see Fig. 1A). PCR was carried out in 96-well optical reaction plates heated to 50 °C for 2 min to digest any dUTP-containing contaminants and to 95 °C for 10 min to deactivate UNG and activate AmpliTaq Gold DNA polymerase, followed by 40 cycles of denaturation at 95 °C for 15 s and annealing and extension at 60 °C for 1 min. Data were analyzed using Applied Biosystems 5700 SEQUENCE DETECTION SYSTEM software.

3. Results and discussion

3.1. Standardization of real-time RT-PCR for detection of BeAn virus RNA

Real-time RT-PCR has supplanted other methods for quantitating RNAs, particularly those of virus RNAs, due to its dynamic range, sensitivity, reproducibility and high throughput (Heid et al., 1996; Morris et al., 1996; McGoldrick et al., 1998; Martell et al., 1999; Lewin et al., 2001; Leutenegger et al., 2001; Oleksiewicz et al., 2001). This assay was standardized and used to detect and quantify TMEV RNA copy equivalents in different parts of the CNS, and to search for potential cryptic extraneural sites of viral persistence in infected mice. To quantify viral RNA copy equivalents in the CNS of TMEV-infected mice, a known quantity of in vitro-transcribed BeAn virus RNA was serially diluted in uninfected mouse brain total RNA, reverse-transcribed and amplified by PCR. All reactions contained equivalent amounts of total RNA to control for primer competition. Mouse brain total RNA alone from uninfected animals served as a negative control. Fig. 1A shows the primer and probe sites on the BeAn virus genome; the majority of the data was acquired with the primers and probe located in the sequences encoding proteins 3B and 3C. The conditions for these primers and probe were optimized for BeAn (see Section 2); the 19-mer probe containing a single nucleotide mismatch with DA virus sequence failed to detect DA virus RNA in infected BHK-21 cells (not shown). Fig. 1B shows

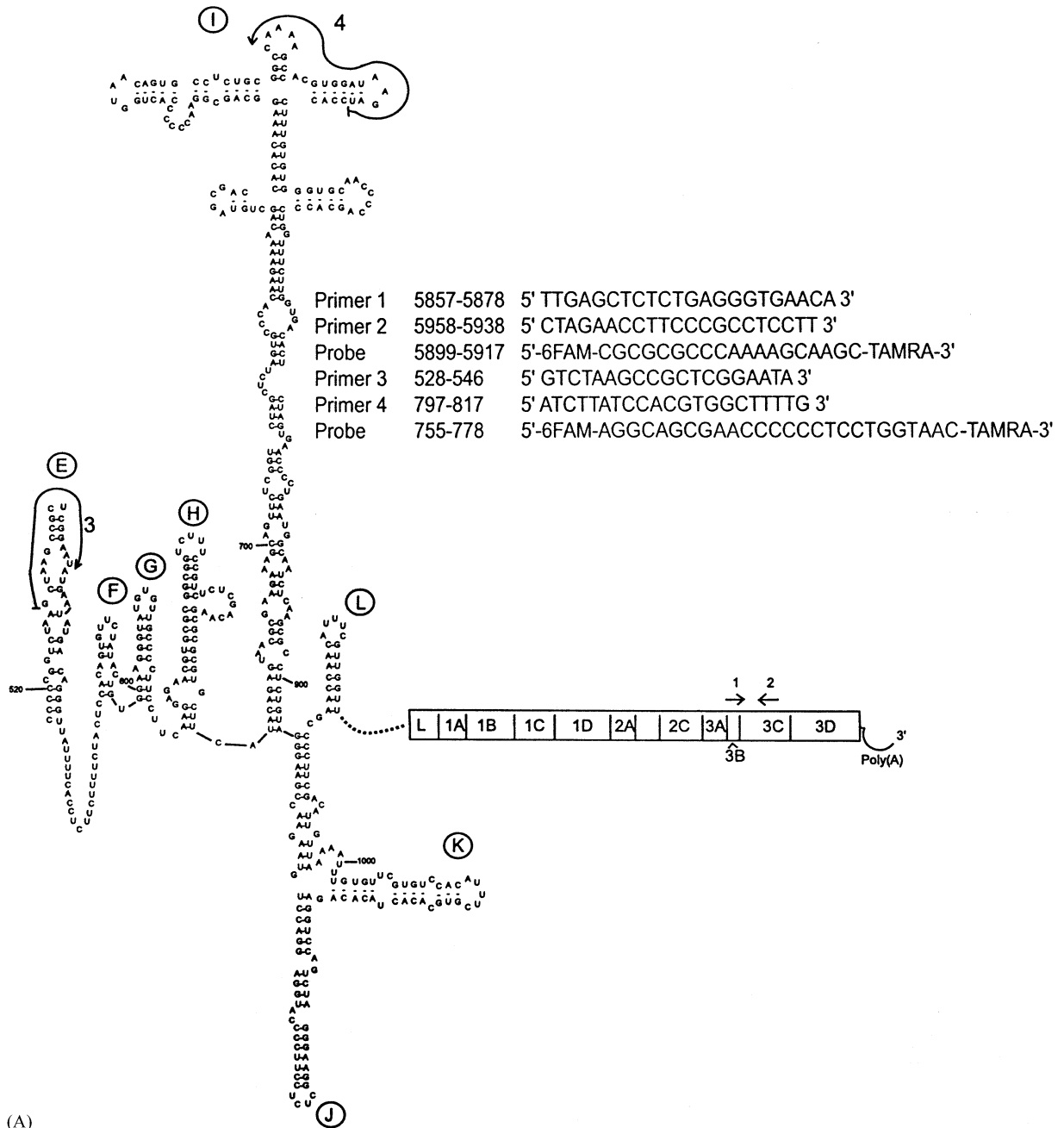
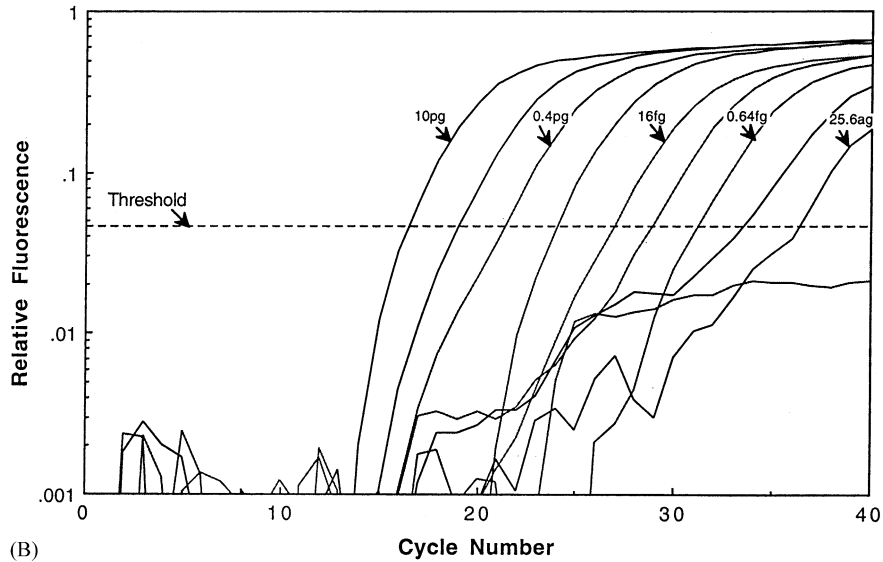
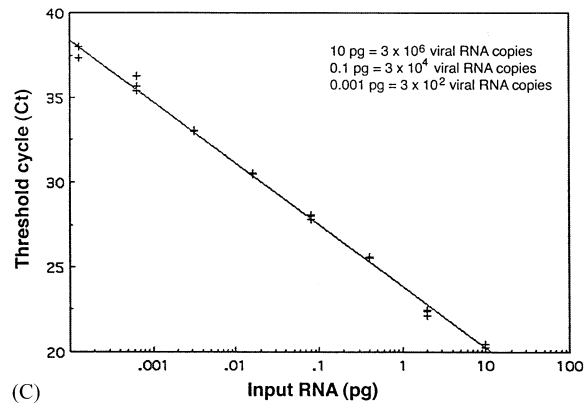


Fig. 1. (A) Location and nucleotide sequence of primers 1 and 2 and probe in sequences encoding proteins 3B and 3C that were specific for BeAn virus and used to obtain most of the data reported below. Another set of primers, 3 and 4, and probe in highly conserved sequences of the internal ribosome entry site in the 5' untranslated region gave similar results and can be used for all TMEV strains. (B) Standardization of real-time RT-PCR for detection of BeAn virus RNA. Plot of relative fluorescence vs. cycle number for RT-PCR reactions of 5-fold dilutions of in vitro-transcribed BeAn RNA from 10 pg to 25.6 ag. Uninfected CNS total RNA served as negative control. The quantity of input BeAn virus RNA in RNA copies is indicated for each plot (1 pg of BeAn RNA 3×10^5 BeAn virus RNA copies). (C) Standard curve generated from real-time RT-PCR of BeAn RNA. The cycle number at which relative fluorescence crossed the threshold for each sample is the Ct value, which is inversely proportional to the amount of BeAn RNA in a reaction. Ct is plotted vs. the amount of BeAn virus RNA in pg. Five-fold dilutions of BeAn virus RNA were analyzed in triplicate and used to construct the standard curve.



(B)



(C)

Fig. 1. (Continued)

amplification plots of normalized fluorescence versus cycle number from a representative experiment. A threshold level above background was arbitrarily assigned based on the intersection with the logarithmic phase of amplification. The cycle number at which relative fluorescence crossed the threshold is referred to as Ct. Thus, the lower the number of BeAn transcripts per reaction, the higher the Ct value. Note that as few as 25 ag of BeAn transcript per reaction was detected, an amount equivalent to approximately eight BeAn virus RNA copies. A standard curve constructed based on the Ct values for each dilution of BeAn

transcript (Fig. 1C) was used to determine virus RNA copy equivalents in mouse tissues. A similar curve was obtained with a different set of primers and probe located in the 5' noncoding region (Fig. 1A) (data not shown).

The sensitivity of this method routinely enabled detection of as few as 20–30 TMEV genomes per μg of total RNA from mouse tissues; thus, real-time RT-PCR is five orders of magnitude more sensitive than the Northern dot blot hybridization we previously used to analyze viral load in spinal cords of TMEV-infected mice (Trottier et al., 2001).

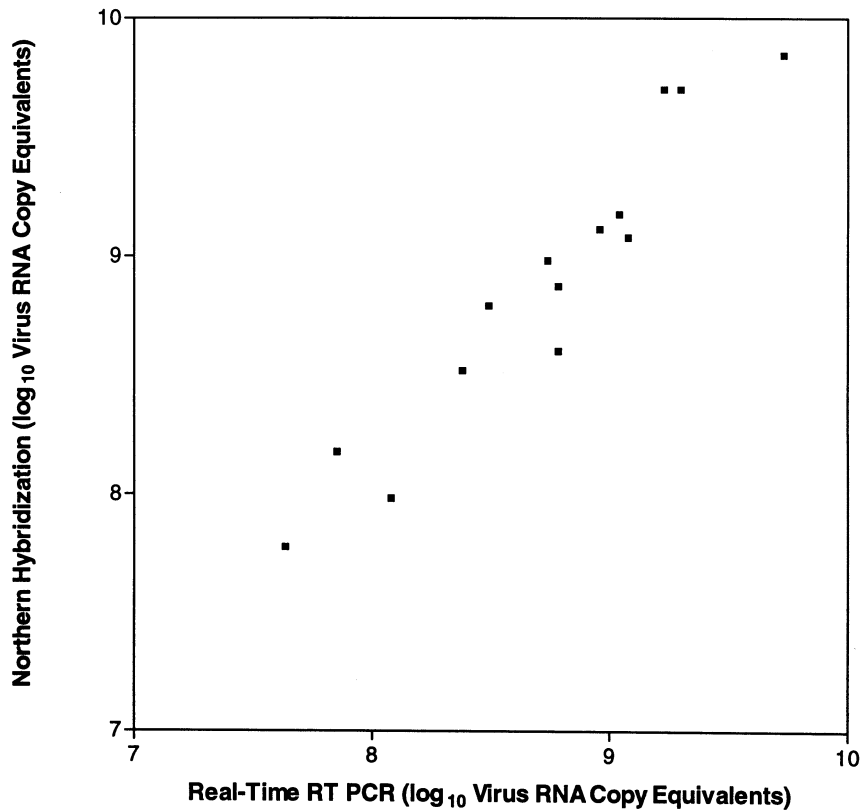


Fig. 2. Comparison of real-time RT-PCR and Northern hybridization in detection of BeAn virus RNA in 14 infected spinal cord total RNA samples containing between 4.3×10^7 and 2×10^9 virus RNA copy equivalents. The *x*- and *y*- axes represent the number of virus RNA copies per spinal cord detected by the respective techniques. The correlation was statistically significant ($r = 0.9052$; $P < 0.001$).

3.2. Correlation between real-time RT-PCR and Northern hybridization detection of BeAn viral RNA copy equivalents in infected mouse spinal cords

The number of virus RNA copies was determined by real-time RT-PCR in a subset of spinal cord total RNA samples previously assayed by Northern hybridization and shown to contain extremely high numbers of virus RNA copy equivalents (Trottier et al., 2001). Real-time RT-PCR was performed using 0.05 or 0.1 μg of infected spinal cord total RNA in reactions with 2.5 μg of uninfected brain total RNA, and compared with a standard curve generated from triplicate samples of in vitro-transcribed BeAn transcripts (Fig. 1C). The TMEV RNA titer for 14 spinal cord samples

ranged between 4.3×10^7 and 2×10^9 copy equivalents. Comparison of the results of real-time RT-PCR with those obtained by Northern hybridization revealed a significant correlation ($r = 0.9052$; $P < 0.001$) (Fig. 2).

3.3. Hierarchy of BeAn virus persistence in the CNS

To assess BeAn virus persistence in the CNS at sites other than the spinal cord, real-time RT-PCR was used to measure BeAn virus RNA copy equivalents in cerebrum, brainstem/cerebellum, spinal cord and CSF. Northern hybridization did not detect virus RNA in the brains of infected mice after the acute phase of infection (not shown). Although, there are virtually no patho-

logical changes in the cerebrum and only minimal changes in the brainstem during demyelinating disease in SJL mice infected with low-neurovirulence TMEV (Lipton, 1975), both sites revealed persisting BeAn virus (Fig. 3). Virus RNA was also detected in the brainstem/cerebellum, presumably representing infection of the brainstem, since no pathological changes have been reported in the cerebellum of persistently infected mice. On average, the number of virus RNA copy equivalents in the spinal cord was 10- and 100-fold higher than in the brainstem/cerebellum and cerebrum, respectively. While virus levels remained relatively constant between 46 and 125 days pi in the brainstem/cerebellum and spinal cord, copy equivalents declined in the cerebrum.

Thus, real-time RT-PCR revealed the primary viral load in the spinal cord, as expected. In spinal cords of persistently infected mice, TMEV RNA and antigens have been found mainly in macrophages (Lipton et al., 1995; Pena Rossi et al., 1997), and to a lesser extent, in oligodendrocytes and astrocytes (Rodriguez et al., 1983; Aubert et al., 1987; Blakemore et al., 1988). The lower BeAn virus RNA copy numbers and lack of continued persistence in the cerebrum, where oligodendrocytes, astrocytes and microglia are plentiful but foamy macrophages are not observed, suggests a fundamental role of foamy

macrophages in perpetuating the infection in the spinal cord, as indicated by experimental depletion of macrophages in infected mice (Pena Rossi et al., 1997). Most foamy macrophages are probably recruited from the periphery rather than arising from resident microglia. The reason for the difference in the recruitment of foamy macrophages into the cerebrum compared with the spinal cord in TMEV infection remains to be elucidated. In order to further define the sites and kinetics of TMEV persistence in the mouse CNS, we have developed methods to isolate relatively pure populations of macrophages and oligodendrocytes from spinal cords of persistently infected mice for viral assays (Trottier et al., 2001). In addition, it is also feasible to use laser capture microdissection of immunostained frozen sections to obtain individual infected cells from a mouse spinal cord (Fend et al., 1999). Since TMEV-infected macrophages and oligodendrocytes in infected spinal cords synthesize on the order of 10^5 viral genomes (Trottier et al., 2001), use of real-time RT-PCR should enable measurement of TMEV RNA copy equivalents in small numbers or even individual cells isolated from the CNS.

Total RNA was also isolated from meningeal and CSF cells, which were present in the effluent after extrusion of cords by forcing PBS into spinal canals, and assayed for the presence of virus RNA

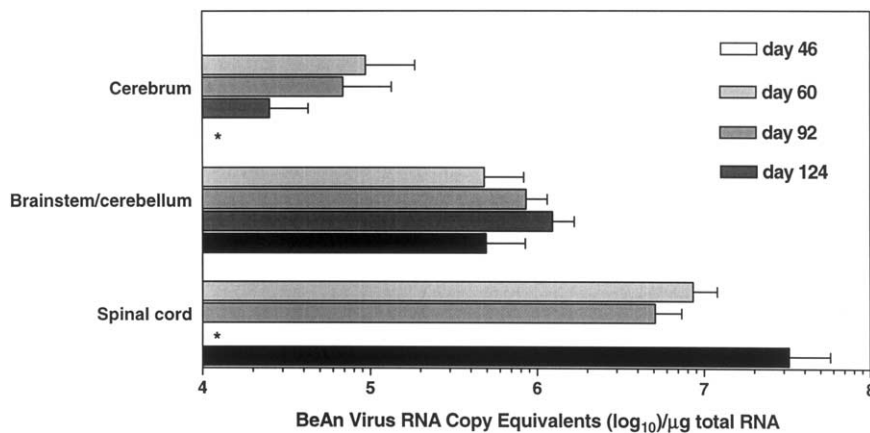


Fig. 3. Persistence of BeAn virus in CNS tissues of infected mice. BeAn virus RNA copy equivalents per μg of total RNA extracted from cerebrum, spinal cord/cerebellum and spinal cord from infected SJL mice was assayed by real-time RT-PCR at different times during the persistent phase of infection. Mean and S.D. values are shown for three to six animals at each time point. Asterisks indicate that samples were not obtained.

copies. Mean copy numbers (\pm S.D.) calculated for the total number of cells collected were $1.07 \pm 0.75 \times 10^7$ ($n = 3$) at day 60 pi and $6.19 \pm 8.62 \times 10^6$ ($n = 4$) at day 92 pi, whereas values for tissues in Fig. 3 are expressed per μg total RNA. Thus, virus RNA copy equivalents were at least 50-fold less abundant in the CSF than in the spinal cord on these 2 days. Nevertheless, BeAn virus RNA copy numbers were higher than expected in the CSF-cell mix. However, quantitative studies of HIV-1 and SIV infections have revealed the presence of high viral RNA loads in CSF. In these retroviral infections, the viral load was 1–2 \log_{10} lower than in plasma, the primary site of viral persistence. In HIV-1 infection, virus RNA copy numbers in CSF correlated well with neurological disease (Cinque et al., 1998; Gisslen et al., 1998; Shepard et al., 2000). In SIV infection of macaques, high levels of CSF virus RNA copies were maintained only in animals developing encephalitis, and antiretroviral compounds that lowered the viral load in CSF delayed the onset of neurological disease (Rausch et al., 1995; Zink et al., 1999). Therefore, it will be important to correlate CSF and spinal cord BeAn virus RNA copy numbers with clinical demyelinating disease in BeAn virus-infected SJL mice.

Real-time RT-PCR was also used to quantitate TMEV genomes in spinal cords of nine infected SJL mice surviving for 9–14 months pi (Table 1). Virus RNA levels declined as the infection progressed; however, 10^5 virus RNA copies per μg of total RNA were detected in spinal cords at approximately 1 year pi. Northern hybridization analysis of virus RNA in four of the nine specimens revealed no virus RNA in the two samples with $< 10^6$ copy equivalents per μg of tissue as detected by the real-time PCR method. This result was expected, because of the lower level of sensitivity of Northern hybridization. Overall, these results suggest that TMEV persists in the spinal cord (and probably the brainstem) of experimentally infected mice for their lifetime, as previously hypothesized (Theiler, 1937; Lipton, 1975), whereas virus is probably eventually cleared from the cerebrum.

Table 1

BeAn virus RNA copy equivalents in the spinal cords of infected

SJL mice at 9–12 months post-infection

Day pi	Real-Time RT-PCR	Northern hybridization
267	2.4×10^7	2.4×10^7
280'1	9.8×10^4	– ^a
280'2	9.4×10^2	–
310	1.4×10^6	3.0×10^6
314	5.0×10^6	nd ^b
322'1	3.0×10^6	nd
322'2	2.6×10^5	nd
359	5.4×10^5	nd
413	3.2×10^5	nd

BeAn virus copy equivalents per μg of total RNA extracted from the spinal cord.

^a Not detected using 10 μg of total RNA for Northern hybridization dot blots.

^b Not done.

3.4. Inability to detect BeAn virus RNA in non-neural tissues during the persistent phase of infection

Information about the sites of viral persistence in a host is crucial for understanding the underlying mechanisms, such as the ability of a virus to evade host immune responses and anti-viral agents. Recent studies of HIV-1 in patients undergoing highly active anti-retroviral therapy have revealed the presence of a second latent viral reservoir harboring replication-competent virus in monocytes, in addition to the known reservoir in resting CD4⁺ T cells (Lambotte et al., 2000). Moreover, other investigations have suggested the presence of another, as yet undiscovered, reservoir of replication-competent virus in HIV-1 infected individuals (Chun et al., 2000; Zhang et al., 2000), underlining the need to identify all sites of HIV-1 persistence. In TMEV persistence, the fact that as much as 5–10% of serum IgG is virus-specific has suggested the existence of an extraneural site of virus replication (Peterson et al., 1992). During acute infections of adult mice, TMEV has a predilection for heart, skeletal muscle and intestine (Olitsky, 1939; Gomez et al., 1996). TMEV has been isolated from the intestinal contents of

mice as late as 2–3 months pi, which may represent delayed viral clearance (Theiler and Gard, 1940). We have been unable to isolate BeAn virus by standard plaque assay or to detect virus antigens by immunofluorescent staining in extraneural organs of infected mice (unpublished data). Shaw-Jackson and Michiel (1999) were unable to detect TMEV in extraneural organs at 6 weeks pi using RT-PCR followed by Southern blotting. Similarly the highly sensitive real-time RT-PCR of total RNA extracted from lung, heart, liver, kidneys, spleen, mesenteric lymph nodes, small intestine, colon, and spinal cord of four BeAn virus-infected SJL mice sacrificed at day 124 pi revealed no BeAn virus RNA in any of the extraneural organs, even when 15 µg of total RNA from tissues was used as template; in these same mice, $> 10^7$ virus RNA copies per µg spinal cord total RNA were detected (not shown). Thus, TMEV persistence appears to be confined to the CNS, at least at 4 months pi. The sequestration of TMEV within the CNS might help it evade host immune responses, with egress of infected CNS macrophages or virions into the peripheral circulation accounting for the abundance of TMEV-specific IgG in serum. Although, not well appreciated, it is theoretically possible for cells and virions to pass from the CSF into venous blood through 7-µm wide fenestra in the arachnoid villi (Tripathi, 1977). It is also believed that lymphocytes and monocytes (possibly infected ones) may possibly exit as they have entered the CNS, through the tight junctions of endothelial cells.

3.5. TMEV infection as a model for a persistent virus infection in MS

TMEV and mouse hepatitis virus infections in mice and Visna virus infection in Icelandic sheep provide relevant experimental animal models for MS (Narayan and Clements, 1989; Lane and Buchmeier, 1997). These animal models represent persistent infections in their natural hosts. Although, experimental infection is induced by ic inoculation, demyelinating disease presumably occurs in nature by the natural route of infection. However, MS is widely believed to be an autoim-

mune disease, triggered by any of several common viruses after an acute or ‘hit-and-run’ infection (Martin and McFarland, 1997). The failure to detect a single MS virus as the cause of this disease in the past half century has in part fueled the belief in an autoimmune basis. Nonetheless, the possibility remains that Multiple Sclerosis (MS) is caused by a single unknown virus with persistent infection driving the immunopathology via CD4⁺ Th1 T lymphocyte responses to virus and not self antigens.

Molecular cloning provides an approach to identifying a virus in MS without prior knowledge of its nature. For example, sera from patients can be used to detect expression of novel viral proteins in a cDNA library. Molecular cloning served in the discovery of hepatitis C virus in humans with non-A, non-B hepatitis virus infection (Choo et al., 1989). It has been assumed that virus RNA replication is restricted during persistent infections of immunocompetent hosts with RNA viruses. This clearly is not the case for persistence of TMEV in mice. Our data on BeAn virus RNA copies in an infected mouse spinal cord might provide a framework for the molecular identification of a persistent virus in MS. Assuming an adult mouse spinal cord contains 5 µg of mRNA (total RNA in cord = 100 µg) and an average mRNA size of 3-kb, the frequency of viral RNA copies in spinal cord lesions during the initial 6 months of infection would be in the range of 1 in 3000 (Fig. 3; Trottier et al., 2001), or on the order of a moderately abundant mRNA. Davidson and Britten (1979) originally described three classes of mRNA abundance for an individual cell; here the classes are applied to multiple cells in an organ system, e.g. CNS. By 1 year of infection and a decline in virus RNA copies, the frequency would be 1 in 300 000 (Table 1) or on the order of a low abundance mRNA. Although, Bureau et al. (1990) reported a comparable low frequency for DA virus clones in a cDNA λ-library made from mouse spinal cord mRNA at 4 months pi, the temporal difference from our predictions may reflect the use of a different TMEV strain in that study and an inoculum ten-fold lower than that in our study. Nevertheless, if the frequency of a virus in an acute MS plaque were

similar to that of a moderately abundant mRNA, as predicted by our study, it would easily fall within the limits of detection by molecular cloning.

Acknowledgements

This work was supported by NIH grant NS 37732.

References

- Aubert, C., Brahic, M., 1995. Early infection of the central nervous system by the GDVII and DA strains of Theiler's virus. *J. Virol.* 69, 3197–3200.
- Aubert, C., Chamorro, M., Brahic, M., 1987. Identification of Theiler's virus infected cells in the central nervous system of the mouse during demyelinating disease. *Microb. Pathog.* 3, 319–326.
- Blakemore, W.F., Welsh, C.J., Tonks, P., Nash, A.A., 1988. Observations on demyelinating lesions induced by Theiler's virus in CBA mice. *Acta Neuropathol.* 76, 581–589.
- Bureau, J.-F., Chirinian, S., Ozden, S., Aubert, C., Brahic, M., 1990. Isolation of a specific cellular mRNA by subtractive hybridization in Theiler's virus persistent infection. *Microb. Pathog.* 8, 335–341.
- Bureau, J.-F., Montagutelli, X., Lefebvre, S., Guenet, J.L., Pla, M., Brahic, M., 1992. The interaction of two groups of murine genes determines the persistence of Theiler's virus in the central nervous system. *J. Virol.* 66, 4698–4704.
- Chamorro, M., Aubert, C., Brahic, M., 1986. Demyelinating lesions due to Theiler's virus are associated with ongoing central nervous system infection. *J. Virol.* 57, 992–997.
- Choo, Q.-L., Kuo, G., Weiner, A.J., Overby, L.R., Bradley, D.W., Houghton, M., 1989. Isolation of a cDNA clone derived from a blood-borne non-A, non-B viral hepatitis genome. *Science* 244, 359–362.
- Chun, T.-W., Davey, R.T. Jr, Ostrowski, M., Justement, J.S., Engel, D., Mullins, J.I., Fauci, A.S., 2000. Relationship between pre-existing viral reservoirs and the re-emergence of plasma viremia after discontinuation of highly active anti-retroviral therapy. *Nat. Med.* 6, 757–761.
- Cinque, P., Vago, L., Ceresa, D., Mainini, F., Terreni, M.R., Vagani, A., Torri, W., Bossolasco, S., Lazzarin, A., 1998. Cerebrospinal fluid HIV-1 RNA levels: correlation with HIV encephalitis. *AIDS* 12, 389–394.
- Clatch, R.J., Lipton, H.L., Miller, S.D., 1986. Characterization of Theiler's murine encephalomyelitis virus (TMEV)—specific delayed-type hypersensitivity responses in TMEV—induced demyelinating disease: correlation with clinical signs. *J. Immunol.* 136, 920–926.
- Davidson, E.H., Britten, R.J., 1979. Regulation of gene expression: possible role of repetitive sequences. *Science* 204, 1052–1059.
- Fend, F., Emmert-Buck, M.R., Chuaqui, R., Cole, K., Lee, J., Liotta, L.A., Raffeld, M., 1999. Immuno-LCM: laser capture microdissection of immunostained frozen sections for mRNA analysis. *Am. J. Pathol.* 154, 61–66.
- Gerety, S.J., Rundell, K.M., Dal Canto, M.C., Miller, S.D., 1994. Class II-restricted T cell responses in Theiler's murine encephalomyelitis virus-induced demyelinating disease. VI. Potentiation of demyelination with and characterization of an immunopathologic CD4⁺ T cell line specific for an immunodominant VP2 epitope. *J. Immunol.* 152, 919–929.
- Gisslen, M., Hagberg, L., Fuchs, D., Norkrans, G., Svennerholm, B., 1998. Cerebrospinal fluid viral load in HIV-1 infected patients without antiretroviral treatment: a longitudinal study. *J. Acquired Immune. Defic. Syndr. Hum. Retrovirol.* 17, 291–295.
- Gomez, R.M., Rinehart, J.E., Wollmann, R., Roos, R.P., 1996. Theiler's murine encephalomyelitis virus-induced cardiac and skeletal muscle disease. *J. Virol.* 70, 8926–8933.
- Heid, C.A., Stevens, J., Litvak, K.J., Williams, P.M., 1996. Real time quantitative PCR. *Genome Res.* 6, 986–994.
- Jarousse, N., Syan, S., Martinat, C., Brahic, M., 1998. The neurovirulence of the DA and GDVII strains of Theiler's virus correlates with their ability to infect cultured neurons. *J. Virol.* 72, 7213–7220.
- Jelachich, M.L., Brumlage, C., Lipton, H.L., 1999. Differentiation of M1 myeloid precursor cells into macrophages results in binding and infection by Theiler's murine encephalomyelitis virus (TMEV) and apoptosis. *J. Virol.* 73, 3227–3235.
- Lambotte, O., Taoufik, Y., deGoer, M.G., Wallon, C., Goujard, C., Delfraissy, J.F., 2000. Detection of infectious HIV in circulating monocytes from patients on prolonged highly active antiretroviral therapy. *J. Acquir. Immune Defic. Syndr.* 23, 114–119.
- Lane, T.E., Buchmeier, M.J., 1997. Murine coronavirus infection: a paradigm for virus-induced demyelinating disease. *Trends Microbiol.* 5, 9–14.
- Larsson-Sciard, E.L., Dethlefs, S., Brahic, M., 1997. In vivo administration of interleukin-2 protects susceptible mice from Theiler's virus persistence. *J. Virol.* 71, 797–799.
- Leutenegger, C.M., Higgins, J., Matthews, T.B., Tarantal, A.F., Luciw, P.A., Pederson, N.C., North, T.W., 2001. Real-time TaqMan PCR as a specific and more sensitive alternative to the branched-chain DNA assay for simian immunodeficiency virus. *AIDS Res. Hum. Retroviruses* 17, 243–251.
- Lewin, S.R., Vesanen, M., Kostrikis, L., Hurley, A., Duran, M., Zhang, L., Ho, D.D., Markowitz, M., 2001. Use of real-time PCR and molecular beacons to detect virus replication in human immunodeficiency virus type 1-infected individuals on prolonged effective antiretroviral therapy. *J. Virol.* 73, 6099–6103.

- Lipton, H.L., 1975. Theiler's virus infection in mice: an unusual biphasic disease process leading to demyelination. *Infect. Immun.* 11, 1147–1155.
- Lipton, H.L., Melvold, R., 1984. Genetic analysis of susceptibility to Theiler's virus-induced demyelinating disease in mice. *J. Immunol.* 132, 1821–1825.
- Lipton, H.L., Twaddle, G., Jelachich, M.L., 1995. The predominant virus antigen burden is present in macrophages in Theiler's murine encephalomyelitis virus-induced demyelinating disease. *J. Virol.* 69, 2525–2533.
- Martell, M., Gomez, J., Esteban, J.I., Sauleda, S., Quer, J., Cabot, B., Esteban, R., Guardia, J., 1999. High-throughput real-time reverse transcription-PCR quantitation of hepatitis C virus RNA. *J. Clin. Microbiol.* 37, 327–332.
- Martin, R., McFarland, H.F., 1997. Immunology of multiple sclerosis and EAE. In: Raine, C.S., McFarland, H.F., Tourtellotte, W.W. (Eds.), *Chapman and Hall Medical*, New York, Multiple Sclerosis: Clinical and Pathogenetic Basis, Churchill.
- McGoldrick, A., Lowings, J.P., Ibata, G., Sands, J.J., Belak, S., Paton, D.J., 1998. A novel approach to the detection of classical swine fever virus by RT-PCR with a fluorogenic probe (TaqMan). *J. Virol. Methods* 72, 125–135.
- Morris, T., Robertson, B., Gallagher, M., 1996. Rapid reverse transcription-PCR detection of hepatitis C virus RNA in serum by using the TaqMan fluorogenic detection system. *J. Clin. Microbiol.* 34, 2933–2936.
- Narayan, O., Clements, J.E., 1989. Biology and pathogenesis of lentiviruses. *J. Gen. Virol.* 70, 1617–1639.
- Oleksiewicz, M.B., Donaldson, A.I., Alexandersen, S., 2001. Development of a novel real-time RT-PCR assay for quantitation of foot-and-mouth disease virus in diverse porcine tissues. *J. Virol. Methods* 92, 23–35.
- Olitsky, P.K., 1939. Viral effect produced by intestinal contents of normal mice and those having spontaneous encephalomyelitis. *Proc. Soc. Exp. Biol. Med.* 43, 434–437.
- Pena Rossi, C., Delcroix, M., Huitinga, I., McAllister, A., van Rooijen, N., Claassen, E., Brahic, M., 1997. Role of macrophages during Theiler's virus infection. *J. Virol.* 71, 3336–3340.
- Peterson, J.D., Waltenbaugh, C., Miller, S.D., 1992. IgG subclass responses to Theiler's murine encephalomyelitis virus infection and immunization suggest a dominant role for Th1 cells in susceptible mouse strains. *Immunology* 75, 652–658.
- Pevear, D.C., Calenoff, M., Rozhon, E., Lipton, H.L., 1987. Analysis of the complete nucleotide sequence of the picornavirus Theiler's murine encephalomyelitis virus indicates that it is closely related to cardioviruses. *J. Virol.* 61, 1507–1516.
- Rausch, D.M., Heyes, M.P., Murray, E.A., Eiden, L.E., 1995. Zidovudine treatment prolongs survival and decreases virus load in the central nervous system of rhesus macaques infected peripherally with simian immunodeficiency virus. *J. Infect. Dis.* 172, 59–69.
- Rodriguez, M., Leibowitz, J.L., Lampert, P.W., 1983. Persistent infection of oligodendrocytes in Theiler's virus-induced encephalomyelitis. *Ann. Neurol.* 13, 426–433.
- Shepard, R.N., Schock, J., Robertson, K., Shugars, D.C., Dyer, J., Vernazza, P., Hall, C., Cohen, M.S., Fiscus, S.A., 2000. Quantitation of human immunodeficiency virus type 1 RNA in different biological compartments. *J. Clin. Microbiol.* 38, 1414–1418.
- Simas, J.P., Fazakerley, J.K., 1996. The course of disease and persistence of virus in the central nervous system varies between individual CBA mice infected with the BeAn strain of Theiler's murine encephalomyelitis virus. *J. Gen. Virol.* 77, 2701–2711.
- Shaw-Jackson, C., Michiel, T., 1999. Absence of internal ribosome entry site-mediated tissue specificity in the translation of a bicistronic transgene. *J. Virol.* 73, 2729–2738.
- Theiler, M., 1937. Spontaneous encephalomyelitis of mice, a new virus disease. *J. Exp. Med.* 65, 705–719.
- Theiler, M., Gard, S., 1940. Encephalomyelitis of mice. I. Characteristics and pathogenesis of the virus. *J. Exp. Med.* 72, 49–67.
- Tripathi, R.C., 1977. The functional morphology of the outflow systems of ocular and cerebrospinal fluids. *Exp. Eye Res.* 25, 65–116.
- Trottier, M., Kallio, P., Wang, W., Lipton, H.L., 2001. High numbers of viral RNA copies in the central nervous system of mice during persistent infection with Theiler's virus. *J. Virol.* 75, 7420–7428.
- Zhang, L., Chung, C., Hu, B.S., He, T., Guo, Y., Kim, A.J., Skulsky, E., Jin, X., Hurley, A., Ramratnam, B., Markowitz, M., Ho, D.D., 2000. Genetic characterization of rebounding HIV-1 after cessation of highly active antiretroviral therapy. *J. Clin. Invest.* 106, 839–845.
- Zink, M.C., Suryanarayana, S., Mankowski, J.L., Shen, A., Piatak, M. Jr, Spelman, J.P., Carter, D.L., Adams, J.D., Lifson, J.D., Clements, J.E., 1999. High viral load in the cerebrospinal fluid and brain correlates with severity of simian immunodeficiency virus encephalitis. *J. Virol.* 73, 10480–10488.